RESEARCH ARTICLE

SABRAO Journal of Breeding and Genetics
55 (4) 1222-1244, 2023
http://doi.org/10.54910/sabrao2023.55.4.17
http://sabraojournal.org/
pISSN 1029-7073; eISSN 2224-8978

MICROMORPHOLOGICAL AND ANATOMICAL RESPONSES OF NATIVE DICOTS TO INDUSTRIAL EFFLUENTS RELEASED FROM CONTAMINATED REGION OF THE CHENAB RIVER IN PAKISTAN

T. ABBAS*, I. AHMAD, Z.I. KHAN, and K. AHMAD

Department of Botany, University of Sargodha, Sargodha, Pakistan
*Corresponding author's email: toqeerabbas01@gmail.com
Email addresses of co-authors: iak8767@yahoo.com, zafar.khan@uos.edu.pk, kafeel.ahmad@uos.edu.pk

SUMMARY

Faisalabad industrial units discharge effluents and associated toxic chemicals into the environment, deteriorating ecological conditions and ecosystem health. Morphoanatomical changes in some medicinally important native species (*Calotropis procera*, *Eclipta alba, Phyla nodiflora,* and *Ranunculus sceleratus*) exposed to heavy industrial pollution gained evaluation. These species of choice were due to their widespread distribution in the area. Ten sites selected in the River Chenab, Chiniot, had three near point source pollution of Faisalabad industries within the 500-m radius (polluted) at three drains and two sites inside the river after each drain point source with the control site at 14 km after from the first industrial drain point source. The general response of all plants to effluents was growth retardation. Plant height increased significantly in all species from river sites. An increase in tallness was more prominent in species like *C. procera* and *P. nodiflora*. An increase in stem sclerification in *C. procera* and *E. alba* from polluted sites occurred, which indicated a better ability to tolerate industrial pollution. Remarkable increases in stem and leaf epidermis, intensive stem sclerenchyma, and closely packed stem vascular bundles in *C. procera* appeared, which could increase resistance to industrial pollution. Most of the morphoanatomical parameters notably attained a decrease in *E. alba*, the most vulnerable species. Plant survival depends on particular structural changes in dermal, mechanical, parenchymatous, and vascular tissues. Overall, industrial pollution adversely impacts plant morphological and micromorphological features, although the reaction of specific species to industrial contamination varies. The study determined that stem and leaf anatomical features, such as, epidermis size and storage tissue thickness, are suitable morphoanatomical markers for industrial pollution biomonitoring. Internal modifications of plants vegetating different industrial contaminated sites played a significant role in high tolerance levels.

Keywords: Industrial pollution, leaf lamina thickness, metaxylem, micromorphology, plant height, sclerification

Key findings: The riparian flora differed significantly across seasons and sites, with substantial micromorphological and anatomical differences. The impact of industrial pollution on the chosen species varied in terms of morphoanatomical parameters.

Citation: Abbas T, Ahmad I, Khan ZI, Ahmad K (2023). Micromorphological and anatomical responses of native dicots to industrial effluents released from contaminated region of the Chenab River in Pakistan. *SABRAO J. Breed. Genet.* 55(4): 1222-1244. http://doi.org/10.54910/sabrao2023.55.4.17.

Communicating Editor: Dr. Himmah Rustiami

Manuscript received: March 30, 2023; Accepted: July 23, 2023.
© Society for the Advancement of Breeding Research in Asia and Oceania (SABRAO) 2023

INTRODUCTION

The textile industry is a chief anthropogenic activity that consumes water and pollutes aquatic bodies (Lellis, 2019). Contamination of marine bodies decreases the freshwater quality and poses a threat to the entire ecology. Given their complicated structures, chemicals from industrial effluents in riverine habitats are hard to neutralize by standard treatments and have a high potential to remain intact in any environment type (Mushtaq *et al.,* 2020). The rising impacts of wastewater released from industries and urban sewage harmfully influence urban streams and rivers. The persistent release of hazardous effluents into the aquatic environment puts at risk the integrity of streams and rivers (Qadir *et al.,* 2008). Different chemicals and phytotoxic contaminants in textile industry wastes significantly affect plant morphological and physiological features (Ho *et al.,* 2012). The large amount of debris and chemicals in industrial polluted water substantially changes plant growth and development (Lokhande, 2011). Species growing in industrially polluted areas are more likely to reflect a high degree of adaptation in their morphology, anatomy, and physiology (Kisku *et al.,* 2000).

This study chose four medicinally significant plant species: *C. procera*, *E. alba*, *P. nodiflora*, and *R. sceleratus*, with selection criteria as follows: (1) natural and widespread species in the region, (2) presence in both pollution-free and industrially contaminated areas, and (3) application in folk medicines because of medicinal importance. Furthermore, the selected species vary significantly in leaf size and texture. *C. procera* is a tall shrub with large fleshy leaves, while *E. alba* leaves in opposing pairs, hairy on both sides, 2–8 cm long, and 5–15 mm broad. *P. nodiflora* and *R. sceleratus* are annual herbs with glabrous leaves that grow up to half a meter tall and have relatively woody rootstock.

Flora's ability to thrive in contaminated environments has plant type, growth characteristics, and leaf morphological traits determining it. The root structure, age and size, and prevalent climatological conditions are essential (Liu *et al.,* 2010). The importance of these characteristics in shaping plant development in a heavily polluted industrial environment brought about a hypothesis that the vegetation that survives under unfavorable conditions must have unique growth and survival processes. As a result, the relevant investigations concentrated on structural and morphological alterations in various sections of selected prominent species. The findings of this study became the basis for analysis of the pollution impacts on plants (ecosystem). The riparian flora of the Chenab River responds differently to various polluted drains for survival under unfavorable conditions.

MATERIALS AND METHODS

Habitat description

The Chenab River flows through a series of dispersed plains and mountains around 46 km from Faisalabad in Pakistan's Punjab province. These plains and mountains, originating in Jammu and Kashmir, cover an area of around 960 km^2. Faisalabad, a metropolis of textile and dying mills and companies involved in printing, weaving, dyeing, and finishing fabrics, is one of Pakistan's most productive hubs.

Experimental sites

Ten choice locations (nine contaminated and one pollution-free) will explore anatomical and morphological aspects of certain dominating species. Choosing the contaminated locations consisted within a 500-meter radius of the polluted region, whereas the industrial pollution-free zone was around 14 km north, near the Chenab Nagar hills. The least amount

of disturbance (human and animal) was a consideration when selecting plant collection sites to ensure the continuous buildup of industrial contaminants at plant growth sites. Every polluted area had different contamination levels because the chief pollutants were distinct.

Climatic conditions

The research region had dry plains and submountain ranges with arid and hot temperatures. The annual average rainfall ranges from 150 to 300 mm, depending on the monsoon precipitation. The typical annual temperature for a selected area is 33 °C, with a mean humidity of 35% and a UV index of seven. (Pakistan Meteorological Department, accessed: March 2019). Plant species collection and observation ensued in all four seasons (winter, summer, autumn, and spring), visiting selected sites 89 times.

Collection and sectioning of plant species

The study included *Calotropis procera*, *Eclipta alba*, *Phyla nodiflora*, and *Ranunculus sceleratus*. Figure 1 depicts a visual picture of the species from contaminated and unpolluted areas. Investigating four plants of average sizes chosen from various study sites proceeded. Gentle removal of plants followed by wrapping in a moist towel preceded transporting to the laboratory for diverse morphological and anatomical characteristics' evaluation. All species' apical internode (2-cm piece) served for stem anatomy, with the fully developed highest leaf chosen for leaf sectioning (a 2-cm slice from the base including midrib). Plant material storage in FAA (formalin acetic alcohol) solution for anatomical research followed a method by Ruzin (1999). Preparing permanent sections used freehand sectioning and staining procedures (Meiji Techno Co., Ltd. Japan). The Model MT4300H Halogen manually calibrated the ocular micrometer with a stage micrometer to examine changes in stem and leaf anatomical properties (size of dermal, parenchymatous, sclerenchymatous, and vascular tissues).

Experimental design and statistical analysis

The experiment progressed in a randomized two-factorial (collection sites and species) setup with six replicates. Mean comparisons used Duncan's multiple range test at a significance threshold of $P \leq 0.05$. Cano Draw v. 4.0, which came with CANOCO for Windows v. 4.5A, served to perform principal component analysis (PCA) and generated biplots.

RESULTS

Morphological parameters

The root length of the four plants investigated had the highest measured at River Site 1 and in drains. The presence of nutrients was responsible for the increase in root length, as the drainage flow rate at these sites was maximum compared with other sites. At the Marala Headworks, the River Chenab provides roughly 25 MAF (30.837225 Km^3) annually and has a higher rainfall-to-snowmelt ratio than the Indus or the Jhelum (Wescoat *et al.,* 2018). According to the presented study, the Marah Chiniot drain has a total flow of 5.19 m^3/s, the Paharang drain of 4.32 m^3/s, and the Ahmad wala drain of 5.90 m^3/s. The root length increased during the spring at all sites compared with other times yearly. The Paharang drain along River Site 1 showed the maximum variation in root length versus the others. Shoot length showed a similar response as root fresh weight to industrial pollution. Marah Chiniot, Paharang and Ahmad wala drains, and River Site 1 all showed significant increases in shoot length in March. High levels of shoot length measurements emerged during spring at the Paharang and Ahmed wala drains and River Site 1 in *C. procera*, *P. nodiflora*, and *R. sceleratus*.

Measuring root and shoot dry weight and total leaf area per plant transpired from fully grown plants. Root and shoot lengths and leaf fresh weight significantly correlate excessively with seasons, sites, and plants (Table 1a). The highest root and shoot lengths occurred in summer (Table 1b). *C. procera*

Figure 1. View of the Chenab River depicting industrial effluents, habitat deterioration, and invading species. S1 (River Site 1, non-polluted), S2 (Marah Chiniot drain), S3 (River Site 2), S4 (River Site 3), S5 (Paharang drain), S6 (River Site 4), S7 (River Site 5), S8 (Ahmad wala drain), S9 (River Site 6), S10 (River Site 7).

Table 1a. Analysis of variance (mean squares) for different morphological characteristics of four ecotypes from 10 sites.

Source of variation	Degrees of freedom	Mean squares		
		Root length (cm)	Shoot length (cm)	Leaf fresh weight (g)
Season (S)	3	252.65**	615.64**	0.0568^{NS}
Site	9	43.08**	143.75**	0.4052**
Plant	3	2645.04**	7765.87**	49.8116**
S × Site	27	11.90^{NS}	41.59^{NS}	0.0486^{NS}
S × Plant	9	41.64**	88.88**	0.0837^{NS}
Site × Plant	27	45.77**	35.13^{NS}	0.3184**
Error	81	11.59	28.20	0.0435
Total	159			

NS = Non-significant ($P > 0.05$); * = Significant ($P < 0.05$); ** = Highly significant ($P < 0.01$).

Table 1b. Comparison of mean with respect to seasons of four ecotypes from 10 sites.

Season	Root length (cm)	Shoot length (cm)	Leaf fresh weight (g)
Spring	12.74±1.40b	27.17±1.88a	0.688±0.156a
Summer	15.01±1.44a	29.01±2.64a	0.746±0.171a
Autumn	13.05±1.48b	24.15±2.07b	0.666±0.152a
Winter	8.99±0.98c	20.03±2.07c	0.734±0.176a

Means sharing similar letter in a column are statistically non-significant ($P > 0.05$).

Table 1c. Comparison of mean with respect to 10 sites of four ecotypes.

Site	Root length (cm)	Shoot length (cm)	Leaf fresh weight (g)
Non polluted	13.92±2.32ab	31.06±4.38a	1.061±0.387a
Marah drain	15.17±2.67a	23.87±3.36bcd	0.799±0.291b
River Site 2	11.22±1.53cd	22.81±3.09cd	0.675±0.229bc
River Site 3	9.34±1.41d	21.15±3.10d	0.709±0.269bc
Paharang drain	11.63±1.40bcd	21.89±3.27d	0.607±0.221cd
River Site 4	12.88±2.86abc	23.62±3.21bcd	0.527±0.194d
River Site 5	11.46±2.19cd	26.36±3.39bc	0.813±0.301b
Ah. wala drain	12.30±2.11bc	25.87±3.11bc	0.688±0.239bc
River Site 6	13.59±2.81abc	27.21±3.07b	0.694±0.254bc
River Site 7	12.99±2.02abc	27.06±5.00b	0.509±0.158d

NS = Non-significant ($P > 0.05$); * = Significant ($P < 0.05$); ** = Highly significant ($P < 0.01$).

Table 1d. Comparison of mean with respect to four plants from 10 sites.

Plant	Root length (cm)	Shoot length (cm)	Leaf fresh weight (g)
C. procera	23.53±1.23a	45.91±1.66a	2.381±0.107a
E. alba	9.74±0.71c	18.32±0.92bc	0.107±0.004c
P. nodiflora	12.34±0.69b	19.51±0.72b	0.208±0.012b
R. sceleratus	4.19±0.25d	16.62±1.10c	0.137±0.005bc

Means sharing similar letter in a column are statistically non-significant ($P > 0.05$).

showed the maximum root length, plant height, and leaf fresh weight at Marah Chiniot drain (Table 1d). The highest root length recorded surfaced at Marah Chiniot drain, with the extensive shoot length recorded at control site in four ecotypes (Table 1c).

Regarding sites and plants in four ecotypes, the highly significant association of leaf dry weight, root fresh weight, and root dry weight was evident (Table 2a). The leaf dry and root fresh weights in four conditions were present and significantly high in summer

Table 2a. Analysis of variance (mean squares) for different morphological characteristics of four ecotypes from 10 sites.

Source of variation	Degrees of freedom	Mean squares		
		Leaf dry weight (g)	Root fresh weight (g)	Root dry weight (g)
Season (S)	3	0.01445**	1.320^{NS}	0.1369**
Site	9	0.00888**	15.499**	0.7614**
Plant	3	0.67948**	806.976**	38.5016**
S × Site	27	0.00266^{NS}	1.459^{NS}	0.0333^{NS}
S × Plant	9	0.01374**	1.317^{NS}	0.0733*
Site × Plant	27	0.00560**	18.717**	0.8476**
Error	81	0.00230	1.199	0.0339
Total	159			

NS = Non-significant ($P > 0.05$); * = Significant ($P < 0.05$); ** = Highly significant ($P < 0.01$).

Table 2b. Comparison of mean with respect to seasons of four ecotypes from 10 sites.

Season	Leaf dry weight (g)	Root fresh weight (g)	Root dry weight (g)
Spring	0.094±0.016b	3.22±0.736a	0.508±0.157b
Summer	0.095±0.018b	3.57±0.746a	0.499±0.148b
Autumn	0.095±0.015b	3.17±0.647a	0.603±0.148a
Winter	0.133±0.030a	3.39±0.737a	0.606±0.166a

Means sharing similar letter in a column are statistically non-significant ($P > 0.05$).

Table 2c. Comparison of mean with respect to 10 sites of four ecotypes.

Site	Leaf dry weight (g)	Root fresh weight (g)	Root dry weight (g)
Non polluted	0.164±0.061a	5.17±1.871a	0.940±0.398a
Marah drain	0.118±0.034b	4.59±1.699ab	0.944±0.405a
River Site 2	0.098±0.025bc	3.21±0.920de	0.461±0.191bc
River Site 3	0.096±0.029bc	4.09±1.339bc	0.586±0.241b
Paharang drain	0.080±0.022c	3.52±1.151cd	0.584±0.242b
River Site 4	0.091±0.027bc	2.48±0.572ef	0.358±0.138c
River Site 5	0.113±0.034bc	2.58±0.881ef	0.419±0.177c
Ah. wala drain	0.095±0.027bc	2.84±0.536def	0.398±0.131c
River Site 6	0.099±0.029bc	2.71±0.847ef	0.451±0.173c
River Site 7	0.090±0.023bc	2.23±0.606f	0.398±0.153c

NS = Non-significant ($P > 0.05$); * = Significant ($P < 0.05$); ** = Highly significant ($P < 0.01$).

Table 2d. Comparison of mean with respect to four ecotypes from 10 sites.

Plant	Leaf dry weight (g)	Root fresh weight (g)	Root dry weight (g)
C. procera	0.300±0.020a	10.00±0.688a	2.025±0.146a
E. alba	0.035±0.002b	1.48±0.173b	0.072±0.012b
P. nodiflora	0.049±0.002b	1.71±0.086b	0.077±0.026b
R. sceleratus	0.035±0.002b	0.17±0.012c	0.041±0.003b

Means sharing similar letter in a column are statistically non-significant ($P > 0.05$).

(Table 2b). Industrial pollution had less impact on species, including *C. procera*, *E. alba*, and *P. nodiflora,* with root and leaf dry weights (Table 2c). *C. procera* showed the maximum leaf dry weight and root fresh, and dry weights versus three environments (Table 2d).

The *C. procera* leaf fresh weight significantly increased in all seasons and locations across four ecotypes. At River Site 1, the maximum leaf fresh weights of *C. procera*, *E. alba*, and *R. sceleratus* were notable in spring. Contrarily, the highest leaf fresh weight

of *P. nodiflora* resulted in Marah Chiniot drain during the summer. The leaf dry weight of *C. procera* proved to be the highest at Chenab Nagar River Site 1 during the winter. The morphological traits, root fresh and dry weights were noticeably highest in *C. procera* in all seasons and Marah Chiniot drain compared with other sites. The root dry weight of all other plants displayed a similar seasonal correlation like the root fresh weight, and little changes in measurement came from the root dry weight of plants (Figure 2).

Morphological comparison of four ecotypes under studied non-polluted, drains, and river sites

A comparison of the mean root length of four ecotypes under the study demonstrated that the root length of *C. procera* was highest in spring and summer at the non-polluted site. Comparing *C. procera* to the other three ecotypes, its average root length consistently displayed the highest values. The shoot length for *C. procera* measured the maximum at a non-polluted site in spring compared with other ecotypes. The shoot length for *C. procera* also appeared significantly high at three drain sites. Compared with other studied plants, the ecotype *C. procera* leaf fresh weight revealed to be the uppermost in spring at River Site 1. Similarly, leaf fresh weight was considerably higher along drains than at other sites for all ecotypes.

The ecotype *Calotropis procera* leaf dry weight had no relation with leaf fresh weight and was the highest in winter at River Site 1 and lowest in autumn at drains. *C. procera* root fresh weight was significantly high at River Site 1 in spring and the high decrease was observed at drains in autumn. Root dry weight of *C. procera*, showed a seasonal correlation with winter. On the other hand, root dry weight characteristics were the same as shown by root fresh weight at non-polluted, drain, and river sites (Figure 3).

Stem anatomical parameters

Stem radius

The stem radius remarkably increased at River Site 6, with the increase in pollution levels, indicating a severe impact of pollution stress on the stem radius. Similarly, the stem radius of *P. nodiflora* also enlarged at Sites 8 and 7. *R. sceleratus* at Site 6 exhibited a notably higher stem radius (Figure 4). Compared with river sites, the stem radius of all plants was considerably smaller in pollution-contaminated areas (Figures 5A, 5B, and 5C).

Dermal tissue

In all plants, epidermal thickness resulted in a meaningful decline in industrially polluted areas. *C. procera* showed an increased stem epidermal cell area at Sites 6 and 10. Furthermore, the *E. alba* stem epidermal cell area was significantly high at Sites 1 and 2. The number of dermal cells increased in *P. nodiflora* stems at Sites 7 and 9. Meanwhile, in *E. alba,* a 5% increase in epidermal thickness emerged at the Paharang drain due to industrial pollution. *R. sceleratus* has a large region of the stem epidermal thickness compared with other plants. The number of epidermal cells in polluted ecotypes is extra low and densely packed.

Parenchymatous tissue

Stem parenchymal thickness exceptionally rose at control and less polluted site (Site 10). Meanwhile, stem parenchyma had decreased at drain sites. Thicker stem parenchyma was visible in *E. alba* at River Sites 2 and 3 compared with drain sites. The thickness of the stem parenchyma in *P. nodiflora* was substantially high at Sites 7 and 9. *R. sceleratus* had an increased parenchyma thickness at Sites 8 and 9. All plant species collected from the industrially contaminated regions had consistently small cortical cell areas because of pollution stress (Figures 5A, 5B, and 5C).

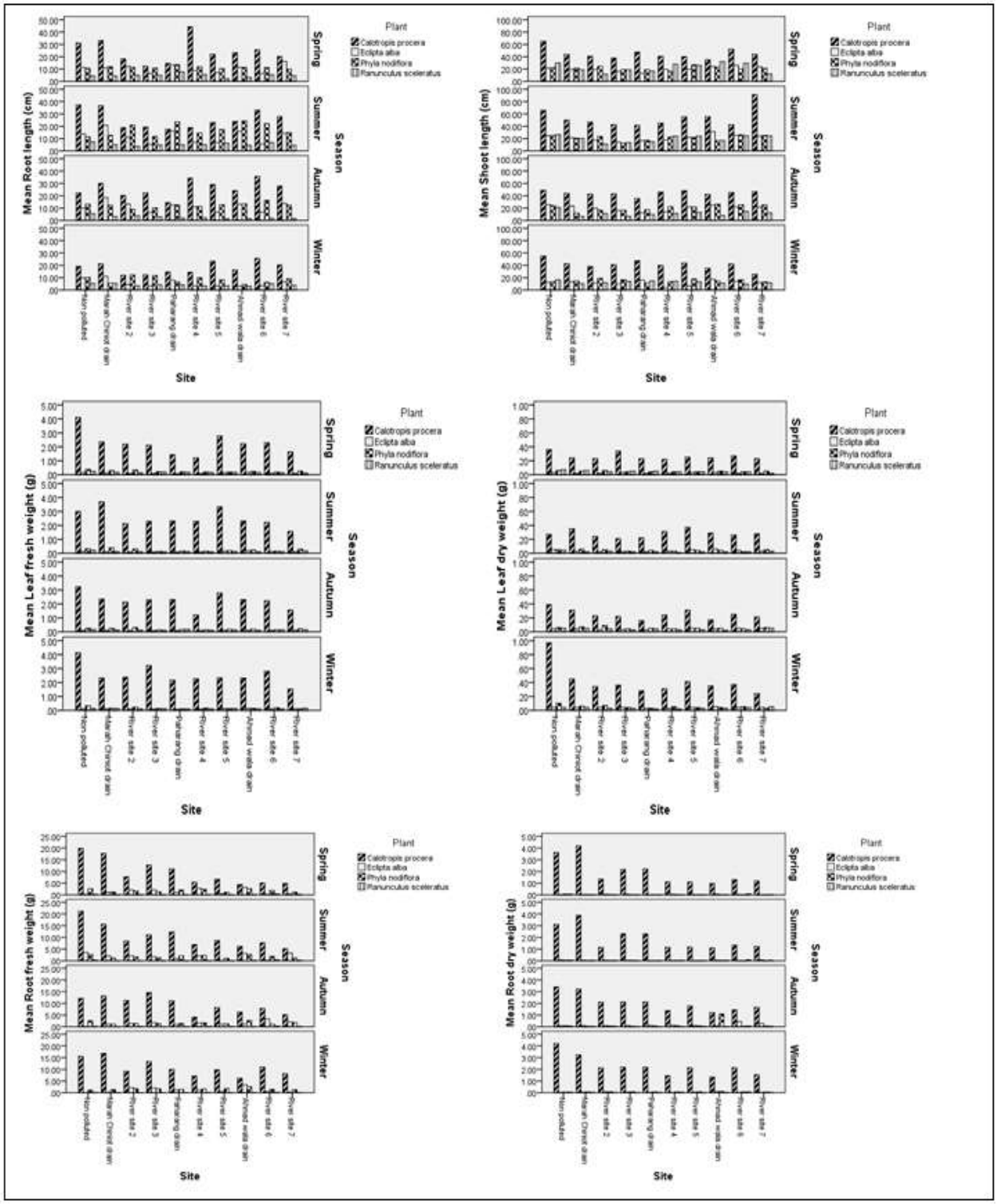

Figure 2. Graph for morphological characteristics in four ecotypes, *C. procera, E. alba, P. nodiflora, and R. sceleratus* in different seasons, March (spring), June (summer), September (autumn), and December (winter) from 10 locations.

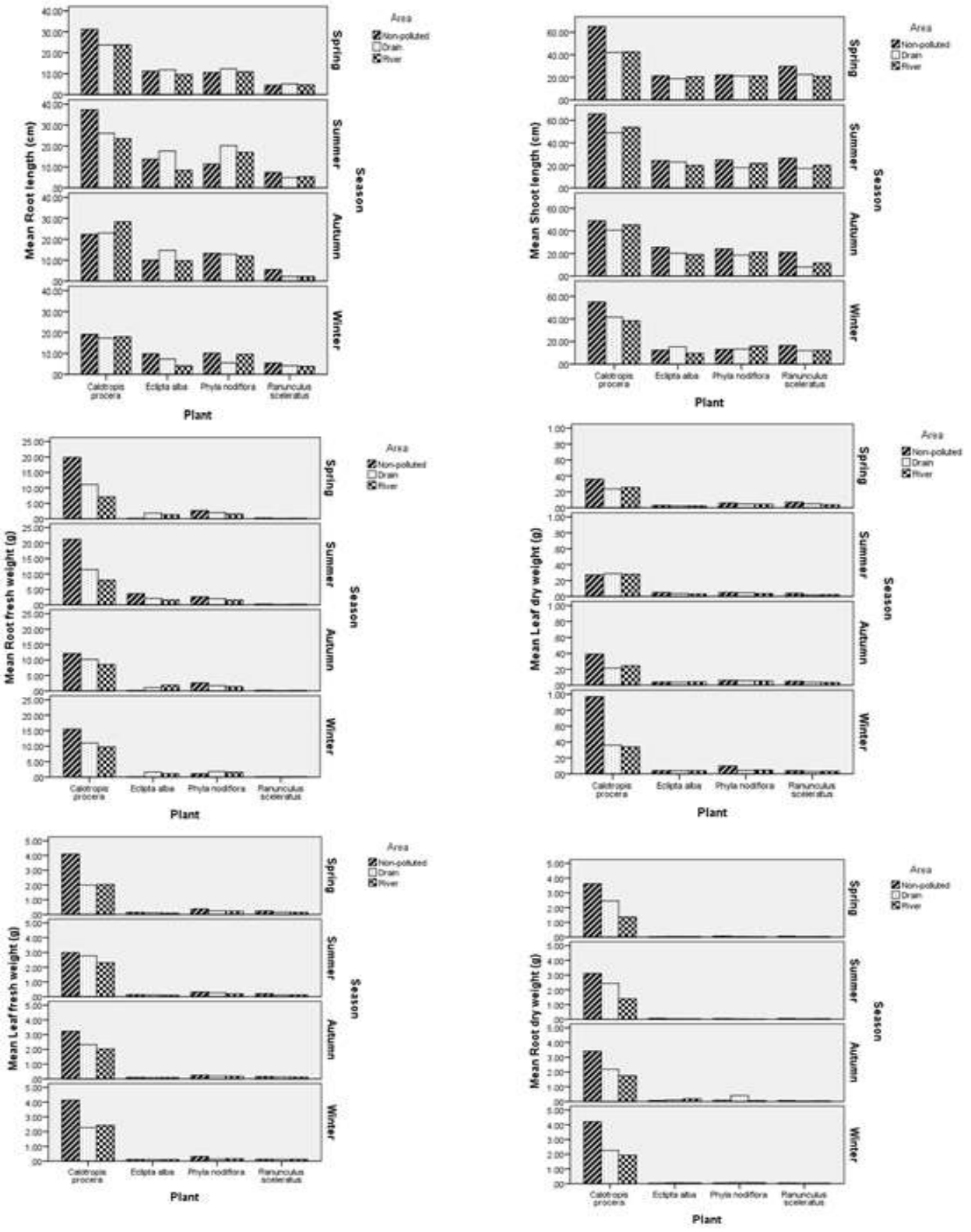

Figure 3. Graph for morphological characteristics in four ecotypes, *C. procera*, *E. alba*, *P. nodiflora,* and *R. sceleratus* in comparison of three areas for different seasons, March (spring), June (summer), September (autumn), and December (winter) from 10 sites.

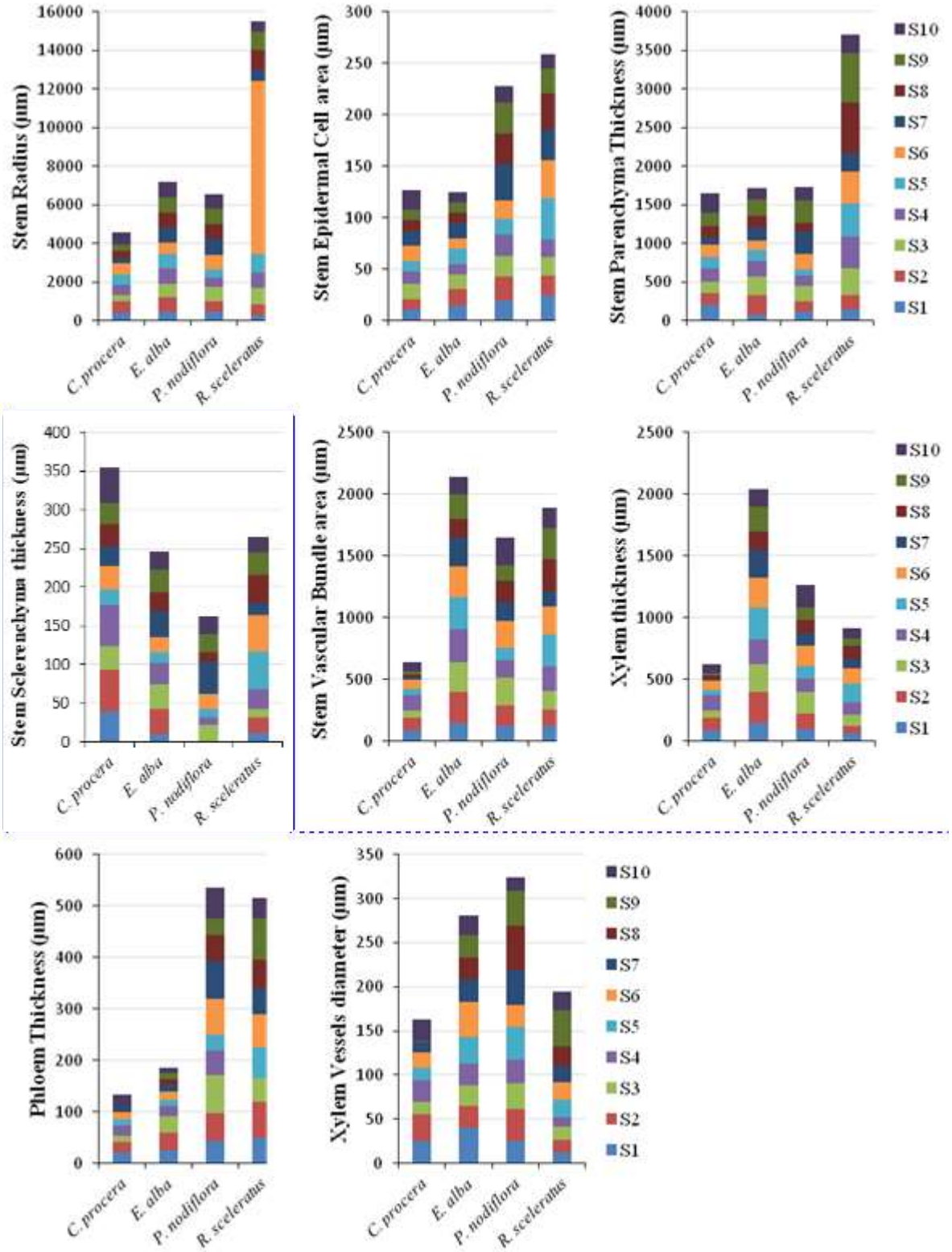

Figure 4. Graphs of stacked clustered bar graphs showing stem anatomical properties of several dicotyledonous species gathered from non-contaminated and industrially polluted areas in River Chenab. Different bar colors refer to different collection sites.

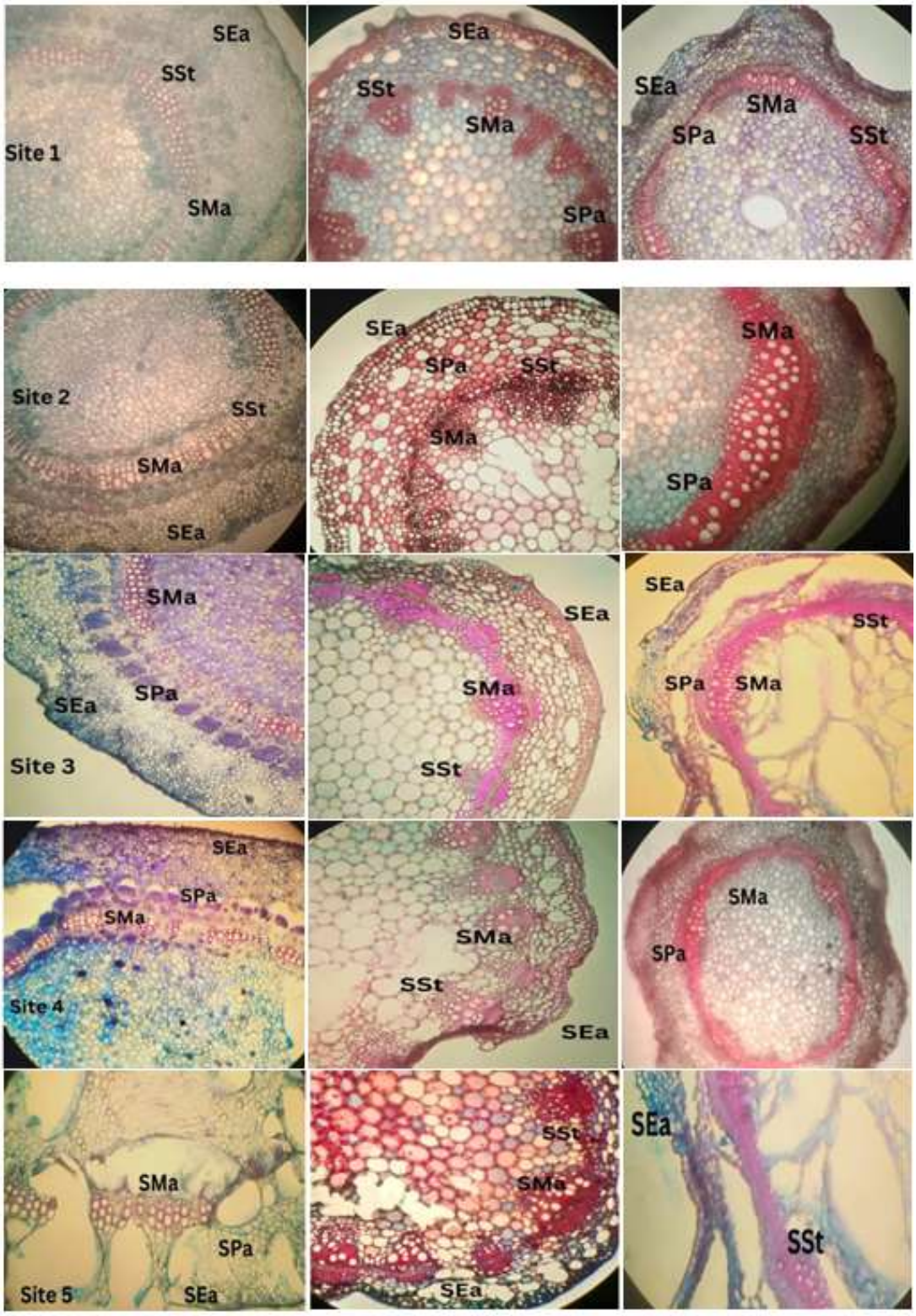

Figure 5(A). Stem anatomy of differently adapted plants (*C. procera, E. alba, and P. nodiflora,* from left to right) from industrially polluted areas. SEa, stem epidermal cell area; SSt, stem sclerenchyma thickness; SMa, stem metaxylem area; SPa, stem parenchyma cell area.

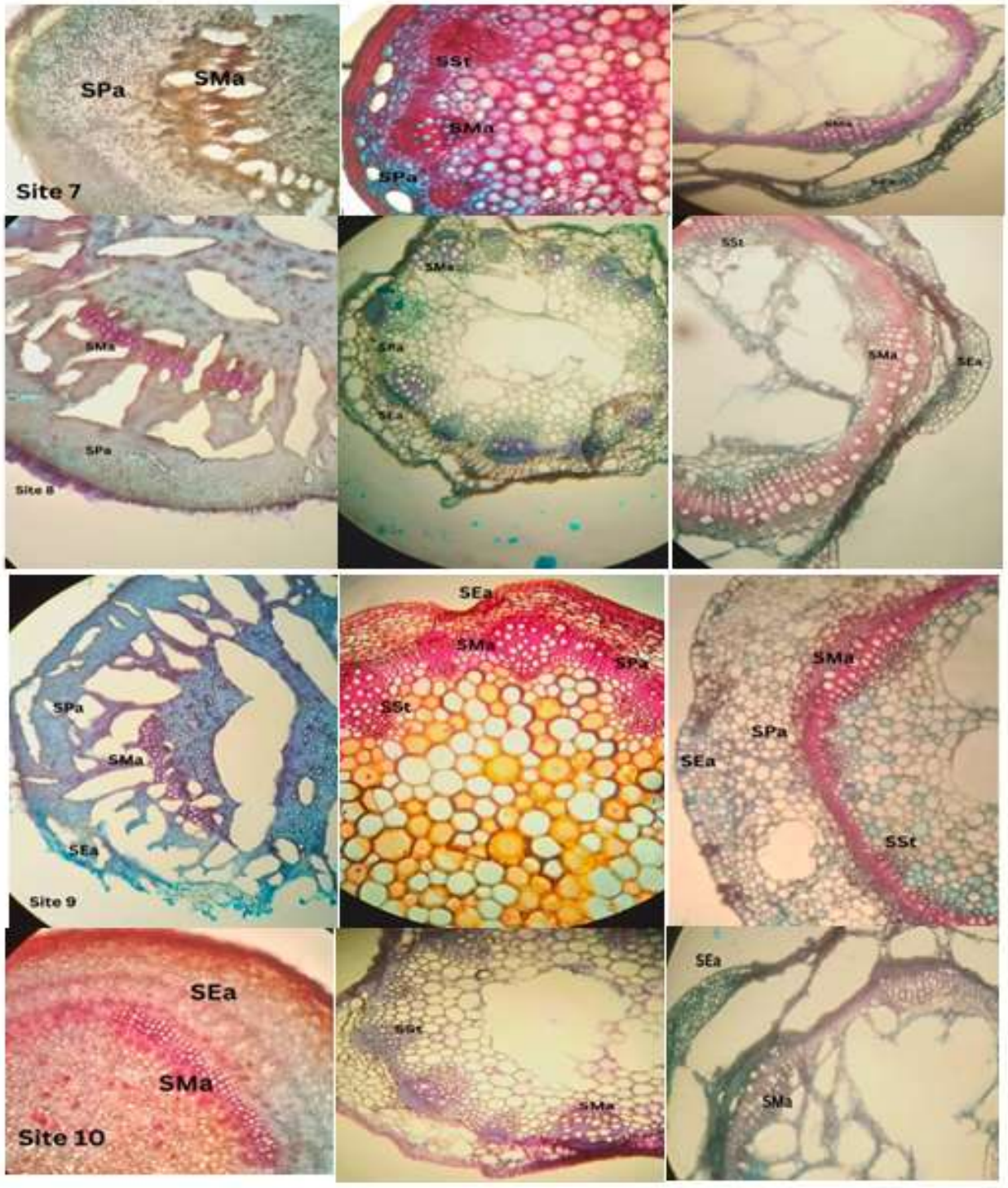

Figure 5(B). Stem anatomy of differently adapted plants (*C. procera, E. alba, and P. nodiflora,* from left to right) from industrially polluted areas. SEa, stem epidermal cell area; SSt, stem sclerenchyma thickness; SMa, stem metaxylem area; SPa, stem parenchyma cell area.

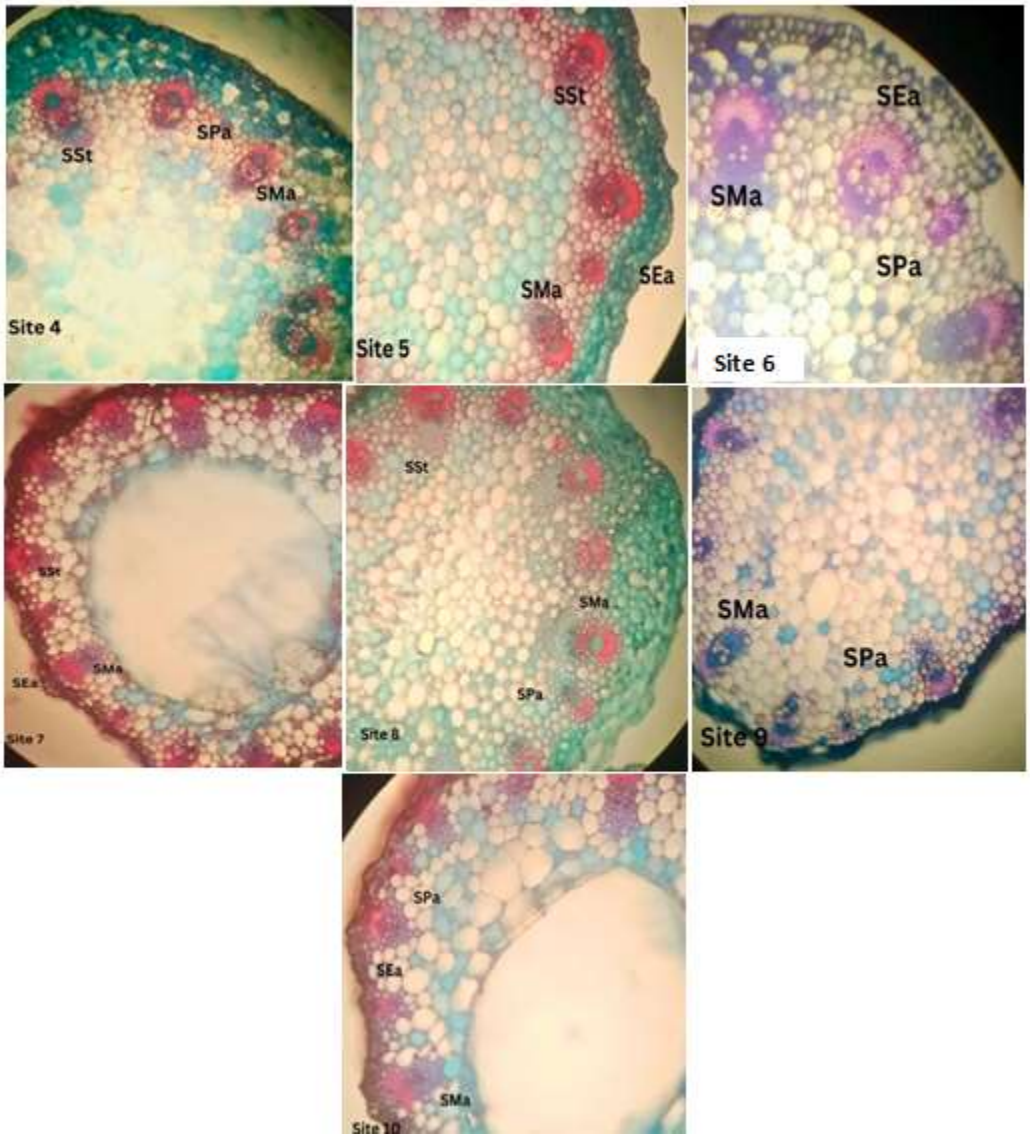

Figure 5(C). Stem anatomy of differently adapted *Ranunculus sceleratus* (Sites 1 to 10) from industrially polluted areas. SEa, stem epidermal cell area; SSt, stem sclerenchyma thickness; SMa, stem metaxylem area; SPa, stem parenchyma cell area.

Sclerenchymatous tissue

The stems of all four plants had the thickest sclerenchyma, and these breadths were greatest at Sites 2, 4, and 10. The denser stem sclerenchyma was noticeable at Sites 2, 3, 7, and 9 in *E. alba*. The sclerenchyma of *P. nodiflora* showed to be the thinnest. Furthermore, sclerenchyma thickness was greater at Site 4 than at the other sites. In assessed ecotypes, *P. nodiflora* and *R. sceleratus* had the thickest stem sclerenchyma at sites 5 and 6 compared with the rest. Pollution increased sclerenchymatous thickness in *R. sceleratus* (Figures 5A, 5B, and 5C).

Vascular tissue

Vascular bundles in the stems of four plants, *C. procera*, *E. alba*, *P. nodiflora*, and *R. sceleratus*, significantly increased at 10 locations. Small vascular bundles occurred as

encircled by a specialized, 5–6 cell thick sclerenchymatous layer at pollution-affected areas. *E. alba* had significantly higher vascular bundles, and *C. procera* had the shortest compared with the other three selected ecotypes. Vascular bundles were most abundant in *P. nodiflora* at Sites 3, 6, and 10. *R. sceleratus* had a very high vascular bundle area at Sites 5 and 9.

Stem xylem thickness

The ecotype *E. alba* has the thickest stem xylem versus *C. procera*, *P. nodiflora*, and *R. sceleratus*. Stem xylem vessels significantly increased at Site 4 in *C. procera*. Furthermore, *E. alba* had the densest xylem vessels compared with the other three ecotypes. At Sites 5 and 6, *E. alba* xylem thickness markedly enhanced. Overall, anatomical parameters of the stem xylem were high at Sites 5 and 6, followed by Site 10.

Stem phloem thickness

In all four studied plants, phloem thickness occurred highest in *P. nodiflora* and lowest in *C. procera*. At Sites 1 and 10, the phloem thickness of ecotype *C. procera* was significantly higher than in other sites. The graph for *E. alba* showed that the phloem area increased at Sites 1, 2, and 3 as pollution stress declined because of the dilution of industrial waste at these sites. The phloem area was also remarkably increased in *P. nodiflora* at Sites 3, 6, and 7 (Figures 5A, 5B, and 5C).

Leaf Anatomical Parameters

Leaf lamina

One of the most striking features is a substantial increase in leaf lamina thickness with an increase in pollution stress. The graphs show (Figures 7A and 7B) that leaf lamina in *C. procera* increased significantly compared with other studied plants. *C. procera* leaf lamina thickness increased at Sites 1, 3, and 4. Similarly, the leaf lamina of *E. alba* indicated consistency across all sites. *P. nodiflora* leaf lamina increased at Site 9 (Figure 6).

Leaf sclerenchyma

At all sites, *C. procera* had the thickest leaf sclerenchyma, and *R. sceleratus* had the thinnest. *C. procera* sclerenchyma thickness occurred significantly high at pollution-affected sites. In *E. alba,* a 10% increase in sclerenchyma thickness happened at the industrially polluted Paharang drain. *P. nodiflora* leaf sclerenchyma rose remarkably at Sites 3, 4, and 5. In contrast, *R. sceleratus* had more sclerenchyma in its leaves at Sites 2 and 9 (Figures 7A, 7B, and 7C).

Leaf lower epidermis

The lower epidermis cell area of the leaf markedly enlarged in *C. procera* and *R. sceleratus* at all sites. A significant increase at the leaf lower epidermis of *C. procera* showed at Sites 5, 4, and 10. The lower epidermis of the leaf vastly increased in *E. alba* at the Paharang and Ahmad wala drains. *P. nodiflora* also showed an increase in the leaf lower epidermis at Sites 10 and 9.

Leaf upper epidermis

The cell area of the upper epidermis of the leaf varied similarly across all sites and ecotypes.

Leaf mesophyll cell area

A maximum mesophyll cell area resulted in *C. procera* and *E. alba* in all sites. *C. procera* had higher levels of leaf mesophyll at Sites 1 and 2. In *E. alba,* a significant increase in leaf mesophyll emerged at Site 7. At Site 5, leaf mesophyll was notably significantly high in *P. nodiflora* (Figures 7A and 7B).

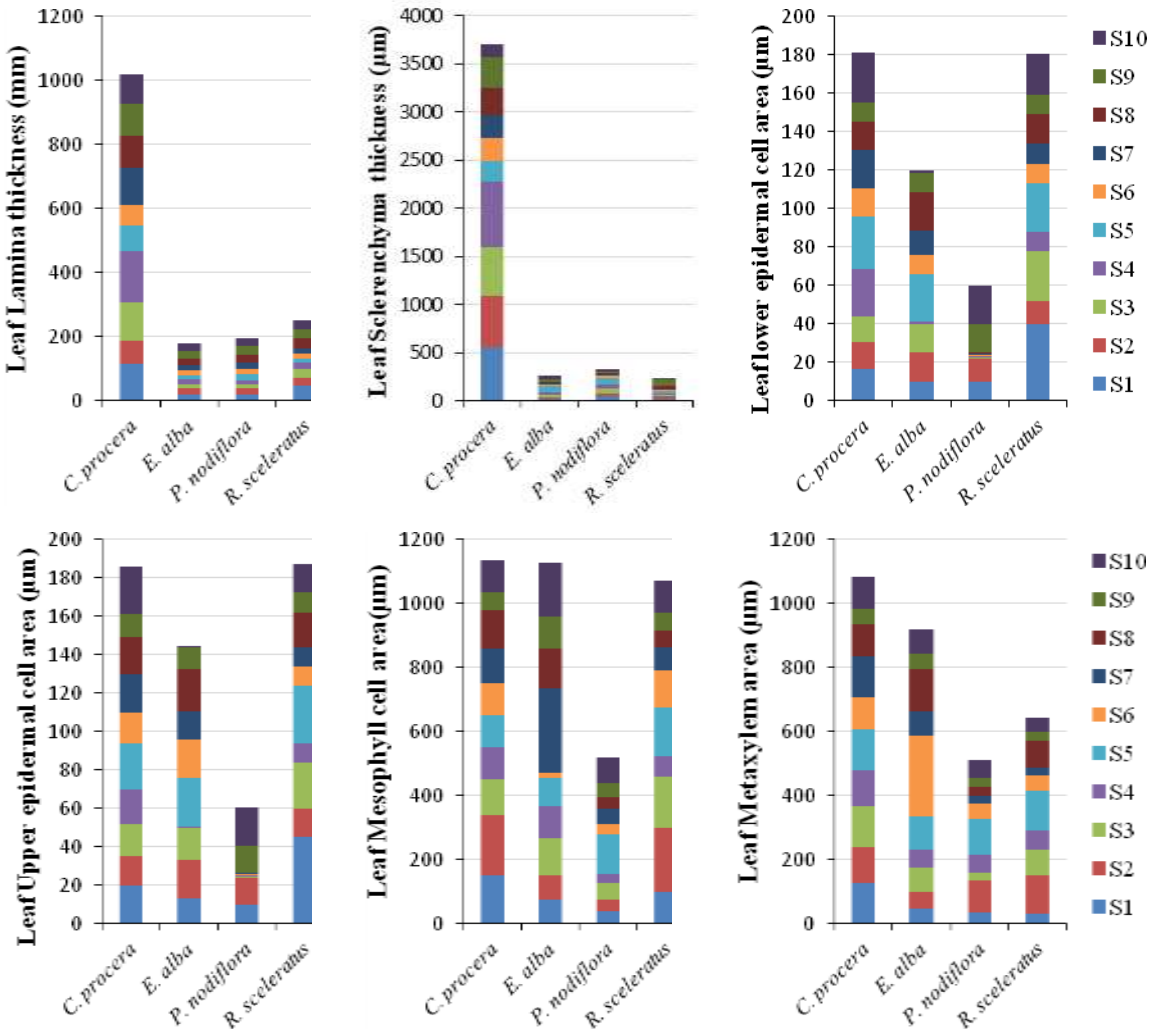

Figure 6. Stacked clustered bar graphs of leaf anatomical characteristics of several dicotyledonous species collected from non-polluted and industrially polluted areas in River Chenab. Different bar colors refer to different collection sites.

Leaf metaxylem

The most increased leaf metaxylem vessel area appeared in *C. procera*, followed by *E. alba*. The leaf metaxylem vessels of *C. procera* were markedly high in all sites except Site 9, which was lower than in other areas. Furthermore, *P. nodiflora* and *R. sceleratus* leaf metaxylem area significantly increased at Marah Chiniot and Paharang drains (Figure 7). Overall, the leaf metaxylem acquired severe impacts at the industrial-contaminated sites compared with non-polluted sites at River Chenab.

Anatomy: stem-leaf correlation

Stem-to-leaf correlations from *C. procera* correlate with seasons and provide clustering in the center. The thickness of the leaf sclerenchyma showed significant relatedness to Site 4, and the thickness of the leaf lamina indicated relatedness to Site 1. Site 2 occurred to be associated with the leaf metaxylem area. For *E. alba*, a biplot of shoot-to-leaf correlation shows that leaf metaxylem area is strongly associated with Site 5, while leaf lamina thickness is deeply associated with Site 9. Site

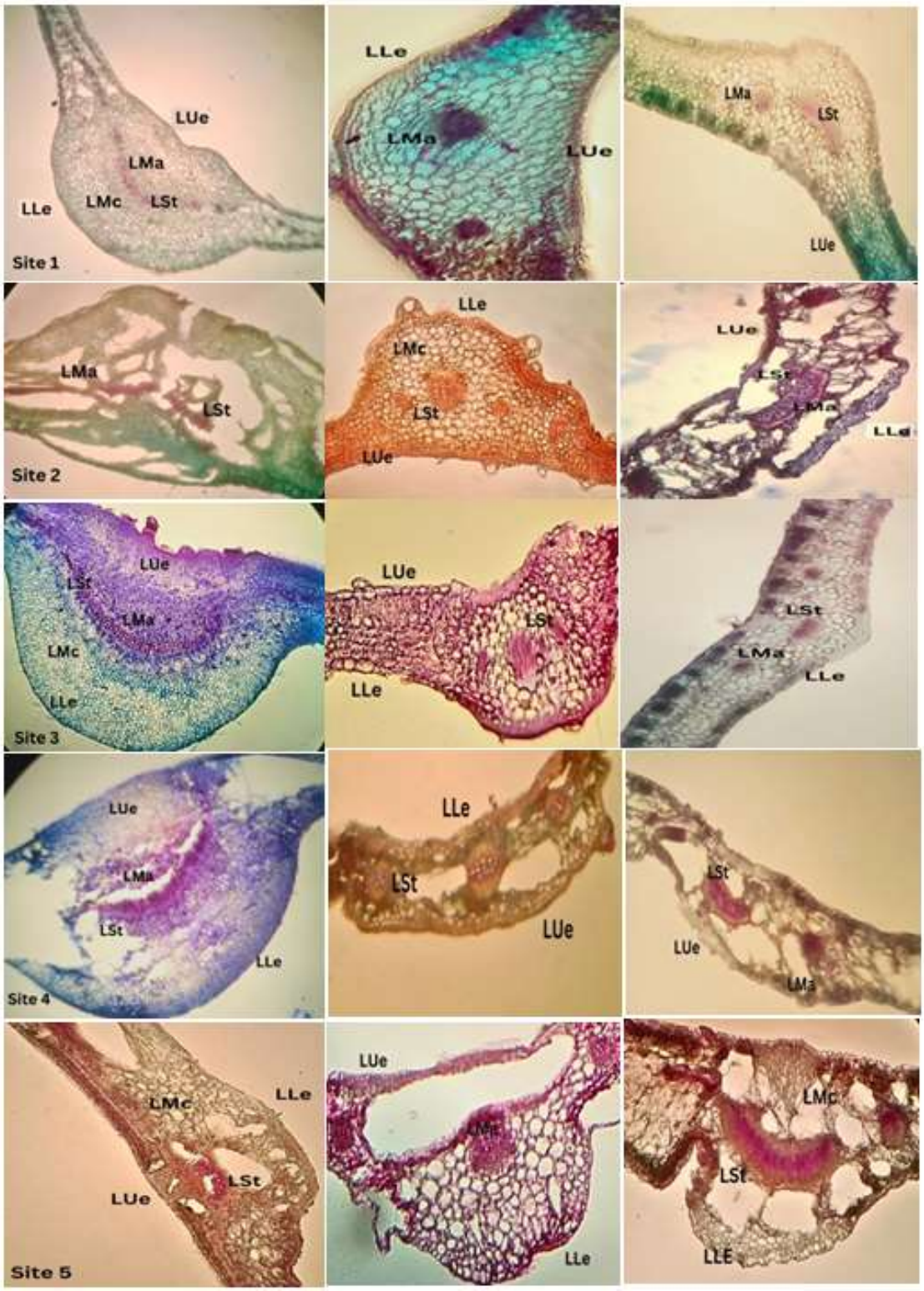

Figure 7(A). Leaf anatomy of differently adapted plants (*C. procera, E. alba, and P. nodiflora,* from left to right) from industrially polluted areas. LLe, leaf lower epidermis cell area; LUe, leaf upper epidermis cell area; LMc, leaf mesophyll cell area; LMa, leaf metaxylem area; LSt, leaf sclerenchyma thickness.

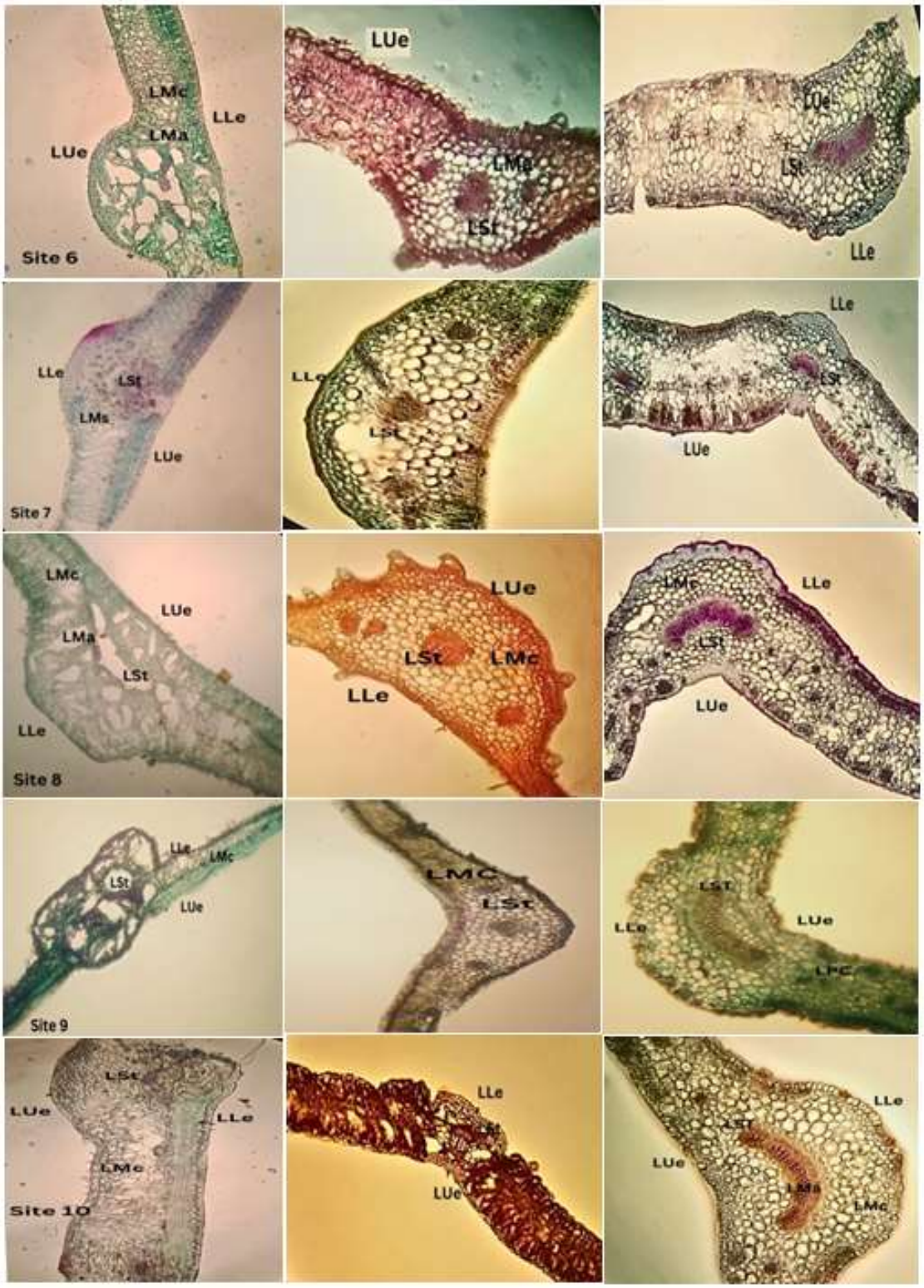

Figure 7(B). Leaf anatomy of differently adapted plants (*C. procera, E. alba, and P. nodiflora,* from left to right) from industrially polluted areas. LLe, leaf lower epidermis cell area; LUe, leaf upper epidermis cell area; LMc, leaf mesophyll cell area; LMa, leaf metaxylem area; LSt, leaf sclerenchyma thickness.

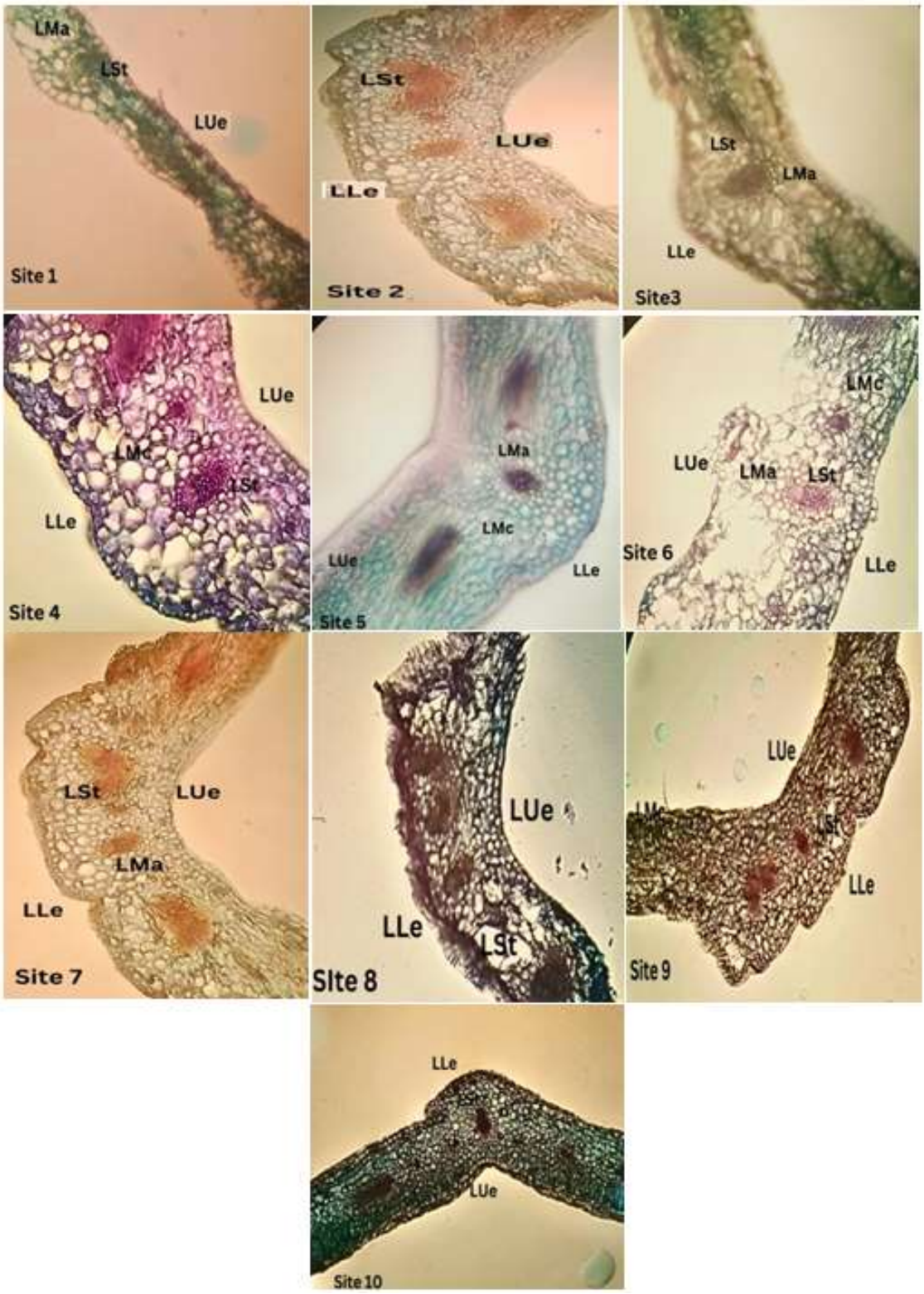

Figure 7(C). Leaf anatomy of differently adapted plant *Ranunculus sceleratus* from industrially polluted areas. LLe, leaf lower epidermis cell area; LUe, leaf upper epidermis cell area; LMc, leaf mesophyll cell area; LMa, leaf metaxylem area; LSt, leaf sclerenchyma thickness.

7 has a strong linkage to the leaf mesophyll area. The stem anatomical structures of *E. alba* had a strong association with sites, concentrating in the center.

P. nodiflora stem-to-leaf correlation biplots differed significantly from the other three plants. Anatomical features of the stem indicated high correlations with the leaf and clustered together. Leaf anatomical structure varied with the stalk, and the leaf metaxylem provided proximity to Site 4. Sites 6 and 10 notably correlated strongly with the lower and upper epidermis of the leaf. The *R. Sceleratus* stem, on the other hand, varied at all locations with the leaf anatomical structures. In *R. sceleratus*, stem structures gave strong associations with Sites 4, 10, and 5, with leaf metaxylem strongly associated with Site 3 (Figure 8).

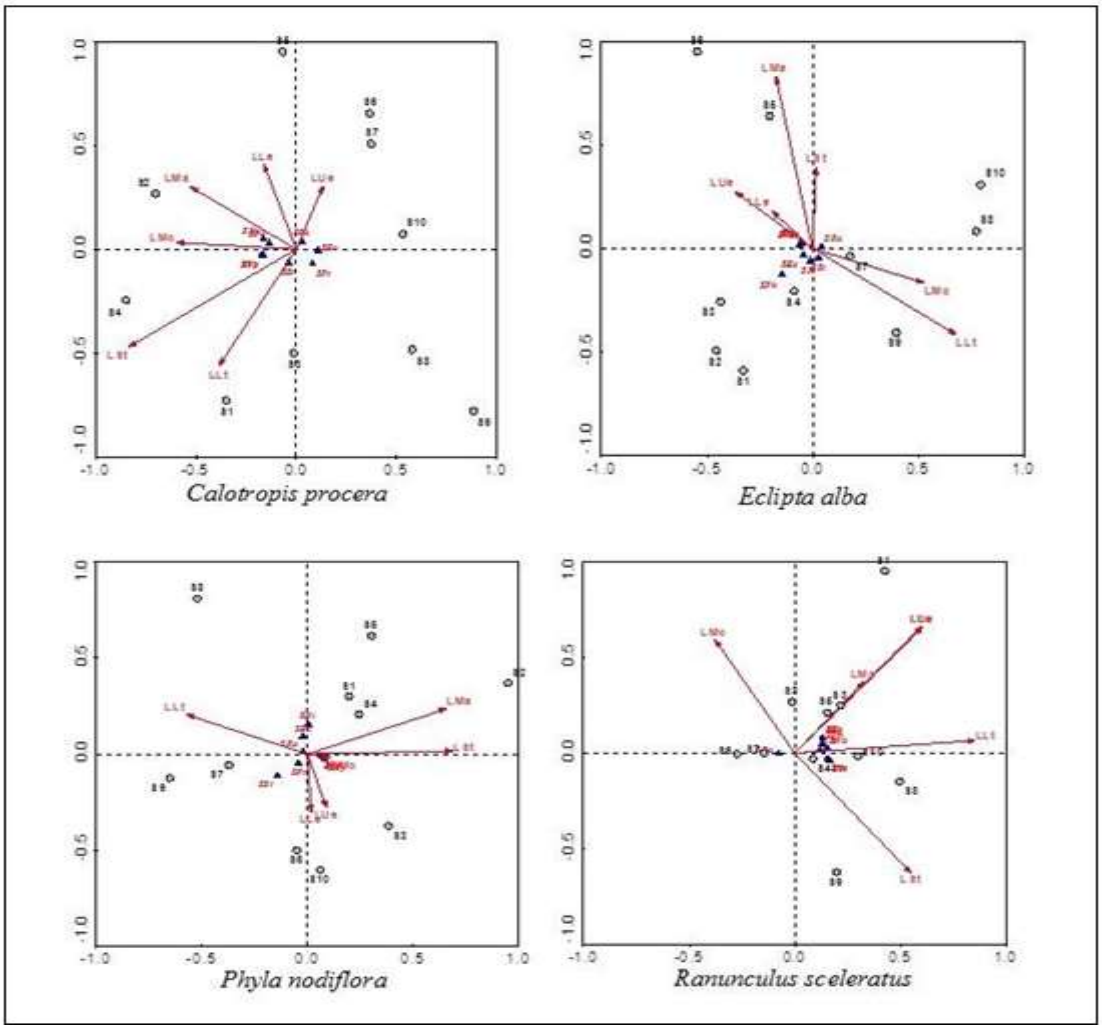

Figure 8. Stem-leaf biplots (Principal Component Analysis) for anatomical attributes of four ecotypes *C. procera*, *E. alba*, *P. nodiflora,* and *R. sceleratus,* showing correlations between industrial polluted and non-polluted areas in drains and River Chenab. Anatomical characteristics: SRa, stem radius; SEa, stem epidermal cell area; SSt, stem sclerenchyma thickness; SMa, stem metaxylem area; SPa, stem parenchyma cell area; SVa, stem vascular bundle area; SPt, stem phloem thickness; LLt, leaf lamina thickness; LSt, leaf sclerenchyma thickness; LLe, leaf lower epidermis cell area; LUe, leaf upper epidermis cell area; LMc, leaf mesophyll cell area; LMa, leaf metaxylem area.

DISCUSSION

Morpho-agronomic characteristics

Investigations on the total plant biomass as root fresh and dry weights, shoot fresh and dry weights, root, and shoot lengths in the four ecotypes *Calotropis procera*, *Eclipta alba*, *Phyla nodiflora*, and *Ranunculus sceleratus* ensued in the presented study. The findings demonstrated that the population varied greatly in the mentioned parameters. Pollution levels in growing areas significantly impacted all the parameters assessed in this study. As a result, all populaces responded differently and did not exhibit any sequence in the results, indicating that three drains, river sites, and non-polluted sites emerged along the River Chenab.

All the species analyzed favored a moderate environment. Morphological features *C. procera* did not vary much over the four seasons. However, it showed a variation at sites and drains, and its population grew with less morphological structure at drains than at river sites, where it flourished the most. Furthermore, except for *C. procera*, reduced fresh weight was detectable in all populations during winter and fall. Aside from *E. alba*, which did not show substantial differences across sites, the rest of the plants showed the same response in all seasons based on morphological features and growth characteristics at River Site 1. At river locations, all plants had an exceedingly substantial beneficial relationship. Kayima *et al.* (2018) and Gales *et al.* (2019) also noted the morphological characteristics of plants at drains and river sites.

Study of morphoanatomical attributes of selected plants

Plants may adapt to numerous stresses by undergoing multiple morphoanatomical changes that have been under study for so long (Hameed *et al.,* 2012; Shehzadi *et al.,* 2019). In this study, several modifications were distinguishable in the stem and leaves of all plants under stress. At polluted sites, sclerification and decreases in parenchyma cell area were the chief modifications in stems. Sclerification, particularly in the vascular region, is the most characteristic response of all plants with increasing altitude (Figures 7 and 8). The sclerenchyma reduction in *C. procera* was visible at all pollution-stressed locations. *R. sceleratus*, which grows in or near water, has the most parenchyma among the plants studied. *P. nodiflora* had less sclerenchyma as it developed away from water sources. The maximum sclerification in the stem was notable in *E. alba* and *C. procera*, demonstrating their ability to adapt to stressful conditions, such as, industrial pollution. *C. procera* stem vascular bundles were significantly lesser than the other three plants due to stress conditions at drains. Under stress circumstances, the plants investigated had the highest levels of aerenchyma. In all four plants, phloem thickness showed the greatest in *P. nodiflora* and the lowest in *C. procera*. *E. alba* provided the thickest stem xylem compared with *C. procera*, *P. nodiflora*, and *R. sceleratus*. According to the current findings, all stem anatomical features had alterations in polluted areas. A typical response in all plants to pollution stress was increasing the intensity of sclerification.

Leaf lamina thickness, leaf upper epidermis, leaf metaxylem, leaf mesophyll cell area, and leaf sclerenchyma thickness occurred to be more susceptible to industrial pollution stress in this study, with substantial changes in response to various types of pollution stresses present in the region. *C. procera* had the thickest leaf sclerenchyma, whereas *R. sceleratus* had the thinnest in all four ecotypes studied. Sclerenchyma thickness enhancement in *C. procera* resulted in Sites 4, 1, 2, and 3. Similarly, *E. alba* had a thickened sclerenchyma at the Paharang drain. *P. nodiflora* leaf sclerenchyma also had augmenting at Sites 3, 4, and 5. *R. sceleratus* had intensive sclerification in its leaves at Sites 2 and 9. *C. procera* and *R. sceleratus* had the maximum leaf lower epidermis cell area, whereas *P. nodiflora* had the lowest. Furthermore, *C. procera* raised the leaf's lower epidermis values at Sites 5, 4, and 10. *C. procera* had the largest leaf metaxylem area, followed by *E. alba*. The value of leaf

metaxylem calculations was the same at all *C. procera* locations except Site 9, where it had declined compared with other sites. The leaf metaxylem in *E. alba* gained enhancement at Site 6, followed by Site 8. The leaf metaxylem of *P. nodiflora* increased at Sites 2 and 5. In all industrially contaminated sites, *R. sceleratus* leaves showed increased metaxylem. It demonstrates that all forms of pollution, particularly industrial effluents, metal toxicity, and nutrient availability, significantly impacted leaf characteristics. Leaf lamina is thicker and intensive sclerification is present in all plants adapted to industrial-polluted areas. Similar findings have come out for numerous plants, where a decline in these characteristics was noticeable in response to many types of stresses, particularly water stress (Chartzoulakis *et al.,* 2002; Guerfel *et al.,* 2009; Hussain *et al.,* 2020; Jan *et al.,* 2022). Higher sclerification of plant leaves was also available at all contaminated locations. Sclerification has grown due to increasing pollution and metal toxicity in the research region. The increased sclerification observed in many studies was due to a response to various kinds of stresses (Rahat *et al.,* 2022; Tufail *et al.,* 2020).

Species with huge leaves, such as, *C. procera* and *P. nodiflora*, are more likely to acquire industrial contamination (Chen *et al.,* 2020). Industrial pollution substantially influenced anatomical traits, especially the size of epidermal cells (Yusypiva and Miasoid, 2019). *C. procera* was the only species whose epidermis, hypodermis, parenchyma, sclerenchyma, and vascular bundle grew in industrially contaminated soil. The thicker epidermis, hypodermis, and sclerenchyma provide mechanical strength and protection for stem-delicate tissues, while the phloem transmits photosynthetic energy (Zoric *et al.,* 2020). These findings showed that increasing *C. procera's* microanatomical traits resulted in a sturdier adaptability to various abiotic stressors (Iqbal *et al.,* 2022; Melo *et al.,* 2021). Except for *C. procera*, the vascular tissue system was typically underdeveloped in all species at the industrially polluted site, as the size of the vascular bundle, metaxylem, and phloem reduced in other species. The increase in vascular tissue visible in *C. procera* under heavy pollution seems implausible, but it appears to relate to the broader, thicker, and more succulent leaves (Ahmad *et al.,* 2021).

The impact of industrial pollution on the chosen species differed in terms of morphological and micromorphological parameters. *C. procera* had more stem and leaf epidermis, sclerenchyma, and vascular bundles, which may improve resilience to industrial pollution and water and nutrient transport. An increase in leaf epidermal thickness and reduced sclerenchyma appeared in *C. procera* and *P. nodiflora*. These species' thicker epidermis may act as a barrier against industrial pollutants. *P. nodiflora* had high stem hypodermal and sclerenchymatous thicknesses, leaf lamina, and leaf sclerenchyma thickness. These characteristics may provide mechanical robustness to stem tissue, enhancing plant survival despite industrial contamination. *E. alba* survival has links to the thick leaf epidermis (both abaxial and adaxial), which might be particularly useful by shielding plants from industrial pollution. Industrial pollution stress severely impacted vascular bundle number, metaxylem, and phloem area, and a variable response of these characteristics were noteworthy in polluted riparian flora.

CONCLUSIONS

The study determined that immense pollution exists at the research locations of River Chenab and three adjacent drains transporting effluents from Faisalabad's industrial region, Punjab, Pakistan. With the enormous existence of effluents along sewers, pollution is prevalent in the form of high metal toxicity. Water and soil quality impairment resulted from increasing wastes from Faisalabad industries to a vast region of drains and the River Chenab. Furthermore, the study indicated that industrial contamination, a foremost contributor to pollution, severely harms the area's natural vegetation. Despite increased contaminant levels, four plants notably flourished at all sites: *C. procera*, *P. nodiflora*, *E. alba*, and *R. sceleratus*. *P. nodiflora* had the maximum flexibility based on proximal activity and

morphoanatomical alterations, followed by *E. alba*. However, due to the considerable imperative value across the research site and a specific morphoanatomical change, all plants investigated have been distinctively the most prevalent acclimatized species of the region, which may benefit industrial pollution revegetation and reclamation.

REFERENCES

Ahmad I, Shamsi L, Hameed M, Fatima S, Ahmad F, Ahmad MSA, Ashraf M, Javaid A, Sultan MA (2021). Micro-morphological response of some native dicotyledonous species to particulate pollutants emitted from stone crushing activities. *Environ. Sci. Pollut. Res*. 28(20): 25529-25541.

Chartzoulakis K, Patakas A, Kofidis G, Bosabalidis A, Nastou A (2002). Water stress affects leaf anatomy, gas exchange, water relations and growth of two avocado cultivars. *Scientia. Hortic*. 95(1-2): 39-50.

Chen B, Xie S, Zhang X, Zhang N, Feng H, Sun C, Lu X, Shao Y (2020). Gut microbiota metabolic potential correlates with body size between mulberry-feeding lepidopteran pest species. *Pest. Manag. Sci*. 76(4): 1313-1323.

Gales JA, Talling PJ, Cartigny MJ, Hughes Clarke J, Lintern G, Stacey C, Clare MA (2019). What controls submarine channel development and the morphology of deltas entering deep-water fjords? *Ear. Surf. Pro. and Landfor*. 44(2): 535-551.

Guerfel M, Baccouri O, Boujnah D, Chaïbi W, Zarrouk M (2009). Impacts of water stress on gas exchange, water relations, chlorophyll content and leaf structure in the two main Tunisian olive (*Olea europaea* L.) cultivars. *Scientia. Hortic*. 119(3): 257-263.

Hameed M, Nawaz T, Ashraf M, Tufail A, Kanwal H, Ahmad MSA, Ahmad I (2012). Leaf anatomical adaptations of some halophytic and xerophytic sedges of the Punjab. *Pak. J. Bot.* 44: 159-164.

Ho YC, Show KY, Guo XX, Norli I, Abbas FA, Morad N (2012). Industrial discharge and their effect to the environment. *Indus. Wast*. 1-33.

Hussain HA, Men S, Hussain S, Zhang Q, Ashraf U, Anjum SA, Ali I, Wang L (2020). Maize tolerance against drought and chilling stresses varied with root morphology and antioxidative defense system. *Plants*. 9(6): 720.

Iqbal U, Hameed M, Ahmad F, Aqeel Ahmad MS, Ashraf M (2022). Adaptive strategies for ecological fitness in (*Calotropis procera* Aiton) WT Aiton. *Ari. Lan. Res. and Manag*. 36(2):197-223.

Jan M, Mir TA, Khare RK, Saini N (2022). Adaptation strategies of medicinal plants in response to environmental stresses. In *Envir. Chall. and Medi. Plants.* 133-151. Springer, Cham.

Kayima JK, Mayo AW, Norbert J (2018). Ecological characteristics and morphological features of the Lubigi Wetland in Uganda. *Envir. Eco. Res.* (4): 218-228.

Kisku GC, Barman SC, Bhargava SK (2000). Contamination of soil and plants with potentially toxic elements irrigated with mixed industrial effluent and its impact on the environment. *Water, air, Soil Poll*. 120: 121-137.

Lellis B, Fávaro-Polonio CZ, Pamphile JA, Polonio JC (2019). Effects of textile dyes on health and the environment and bioremediation potential of living organisms. *Biotechnol. Rese. Inn*. 3(2): 275-290.

Liu Y, Zeng G, Wang X, Chen B, Song H, Xu L (2010). Cadmium accumulation in *Vetiveria zizanioides* and its effects on growth, physiological and biochemical characters. *Biore. Tech*. 101(16): 6297-6303.

Lokhande RS, Singare PU, Pimple DS (2011). Study on physico-chemical parameters of waste water effluents from Taloja industrial area of Mumbai, India. *Int. J. Eco*. 1(1): 1-9.

Melo AS, Yule TS, Barros VA, Rivas R, Santos MG (2021). C3-species *Calotropis procera* increase specific leaf area and decrease stomatal pore size, alleviating gas exchange under drought and salinity. *Acta Physiol. Plant*. 43(11): 1-11.

Mushtaq N, Singh DV, Bhat RA, Dervash MA, Hameed OB (2020). Freshwater contamination: Sources and hazards to aquatic biota. In *Fres. Wat. Poll. Dyn. Reme.* 27-50.

Qadir A, Malik RN, Husain SZ (2008). Spatio-temporal variations in water quality of Nullah Aik-tributary of the river Chenab, Pakistan. *Environ. Monit. Asses.* 140(1): 43-59.

Rahat QUA, Hameed M, Fatima S, Ahmad MSA, Ashraf M, Ahmad F, Khalil S, Munir M, Shah SMR, Ahmad I, Younis A (2022). Structural determinants of phytoremediation capacity in saltmarsh halophyte (*Diplachne fusca* L. P. Beauv. ex Roem. & Schult. subsp. Fusca). *Int. J. Phytorem.* 1-16.

Shehzadi A, Akram NA, Ali A, Ashraf M (2019). Exogenously applied glycinebetaine induced alteration in some key physio-biochemical attributes and plant anatomical features in water stressed oat (*Avena sativa* L.) plants. *J. Arid Land*. 11(2):292-305.

Tufail A, Aqeel M, Khalid N, Ahsan M, Khilji S, Ahmad F, Hashem M (2020). Salt toxicity in a natural habitat induces structural and functional modifications and modulate metabolism in Bermuda grass (*Cynodon dactylon* [L.] Pers.) ecotypes. *Appl. Ecol. Environ. Res*. 18(5): 6569-6588.

Wescoat JL, Siddiqi A, Muhammad A (2018). Socio-hydrology of channel flows in complex river basins: Rivers, canals, and distributaries in Punjab, Pakistan. *Water Resour. Res.* 54(1): 464-479.

Yusypiva T, Miasoid H (2019). The state of bio-ecological characteristics of the one-year shoots of *Robinia pseudoacacia* L. under the conditions of industrial pollution. *Ekol*. 38(3): 240-252.

Zoric L, Milic D, Karanovic D, Lukovic J (2020). Anatomical adaptations of halophytes within the Southern Pannonian Plain Region. *Handbook of Halophytes: Mol. Eco. Biol. Agric*. 1-27.